NAS Technical Report; NAS-06-009
August 2006

Molecular Data for a Biochemical Model of DNA Damage: Electron Impact Ionization and Dissociative Ionization Cross Sections of DNA Bases and Sugar-Phosphate Backbone

Winifred M. Huo[1], Christopher E. Dateo[2] and Graham D. Fletcher[2,3]

NASA Ames Research Center, Mail Stop T27B-1, Moffett Field, CA 94035-1000, USA

Abstract

As part of the database for building up a biochemical model of DNA radiation damage, electron impact ionization cross sections of sugar-phosphate backbone and DNA bases have been calculated using the improved binary-encounter dipole (iBED) model. It is found that the total ionization cross sections of C_3'- and C_5'-deoxyribose-phosphate, two conformers of the sugar-phosphate backbone, are close to each other. Furthermore, the sum of the ionization cross sections of the separate deoxyribose and phosphate fragments is in close agreement with the C_3'- and C_5'-deoxyribose-phospate cross sections, differing by less than 10%, an indication that a building-up principle may be applicable. Of the four DNA bases, the ionization cross section of guanine is the largest, then in decreasing order, adenine, thymine, and cytosine. The order is in accordance with the known propensity of oxidation of the bases by ionizing radiation. Dissociative ionization (DI), a process that both ionizes and dissociates a molecule, is investigated for cytosine. The DI cross section for the formation of H and $(\text{cytosine-H1})^+$, with the cytosine ion losing H at the 1 position, is also reported. The threshold of this process is calculated to be 16.9 eV. Detailed analysis of ionization products such as in DI is important to trace the sequential steps in the biochemical process of DNA damage.

[1] Corresponding author, whuo@mail.arc.nasa.gov
[2] ELORET Corp., Sunnyvale, CA, USA
[3] Now at CCLRC Daresbury Laboratory, Daresbury, Cheshire, WA4 4AD, UK

1. Introduction

In radiation research, a biophysical model is frequently used to link the dosimetry of radiation with measurements of biological damages. Based on a stochastic approach and employing empirical data of energy deposition and molecular damage, Monte Carlo simulation has evolved to the stage that it has become an important tool in the modeling and calculation of initial effects of radiation damage (*1,2*). Simultaneously, advances in experimental techniques have begun to provide information on the chemical processing that links the early physical events to the biological damage evolved later. It is therefore desirable to extend the modeling so as to provide the framework for analyzing such experimental data. So far, virtually all analyses of chemical processes are based on energetic considerations. More rigorous theoretical analysis, involving quantitative estimates of damage probability, is desirable. Such a model can be employed to understand not just the damage mechanism, but also the repair mechanism, and to propose possible countermeasures.

Due to the lack of atomistic detail, Monte Carlo track simulations cannot be easily adapted to include chemical processes. A detailed biochemical model that includes explicit chemical structures offers an alternate approach. In a biochemical model, it is not only necessary to know the initial energy deposition and probability of damage, but also the chemical identity of the damage products so that it can predict the subsequent steps of the damage process. Chemical structures are an integral part in the simulation. Detailed microscopic data, including electron (δ-ray) collision cross-sections, chemical reaction rates, and transport properties, are needed for the modeling. So far only limited data are available.

The role of ionization in DNA damage is well recognized. The ionization (oxidation) of the 2'-deoxy-D-ribose sugar (abbreviated as deoxyribose below) results not only in strand breaks, but also in the formation of a variety of electrophilic degradation products that can further react with proteins and DNA bases (*3*). The guanine radical cation is considered one of the precursors to the primary, direct-type lesions formed in DNA when it is irradiated *in vivo* (*4*). Up to the present, no experimental measurement of the cross sections of these moieties has been reported. On the theoretical side, Bernhardt and Paretzke (*5*) calculated total ionization cross

sections for the DNA and RNA bases and sugar-phosphate backbone using both the semiclassical Deutsch-Märk (DM) formalism (*6*) and the Binary-Encounter Bethe (BEB) formalism of Kim and Rudd (7). Note, however, that the ribose group in their sugar-phosphate calculation replaces two OH groups in deoxyribose by H (*8*) and thus should be considered an analog of the deoxyribose-phosphate fragment. Mozejko and Sanche (*9*) reported BEB cross sections for the total ionization of the four DNA bases and the RNA base uracil. BEB cross sections of selected analogs of the sugar phosphate backbone have also been calculated (*10*). So far studies using the more recently developed improved binary-encountered dipole (iBED) formalism (*11*) are not yet available. Furthermore, dissociative ionization (DI), a process that simultaneously ionizes and dissociates a molecule, has never been used in analyzing direct DNA damage, in spite of the fact that the OH radicals generated by the DI of water plays an important role in indirect damage mechanisms. As part of the molecular database to build up a biochemical model, this paper reports total ionization cross sections, $M + e \rightarrow 2e$ + all products, for deoxyribose, phosphate, C_3'- and C_5'-deoxyribose-phosphate, and the four DNA bases using the iBED formalism. The total ionization cross section describes the probability of depositing electron energy on the target molecular species, producing a new electron. It does not provide the information regarding the nature of the molecular damage. To obtain details of the damage, studies of processes such as DI are required. The first study of DI of a DNA base is also presented here.

2. Method and Materials

Quantum mechanical methods have been used to calculate the electron impact ionization cross sections of small functional groups of DNA: deoxyribose, phosphate, C_3'- and C_5'-deoxyribose-phosphate, and the four DNA bases guanine, adenine, thymine, and cytosine. The corresponding quantity for water was also calculated. The same methodology was used to study the DI of cytosine. In all cases, the calculations were performed for the isolated molecules, not as part of the DNA. Similarly, water was treated as an isolated molecule.

The calculation of electron impact ionization cross sections involves the following steps:

(a). Calculation of the equilibrium geometry of biomolecules

While the equilibrium geometry of the water molecule is known well both experimentally and theoretically, the equilibrium geometries of isolated DNA functional groups are not as well established. No experimental data are available for the isolated molecules and previous theoretical studies (*5,9*) used the low-order Hartree-Fock (HF) method (*12*) and smaller basis sets in the geometry optimization. In this study, the second-order Møller-Plesset perturbation theory (MP2), a standard quantum chemistry method that includes treatment of electron correlation (*12*), was used to determine the equilibrium geometry. All geometry calculations were carried out using the correlation-consistent-polarized valence double zeta (cc-pVDZ) basis set of Gaussian functions (*13-15*).

(b). Calculation of the kinetic energies and ionization potentials of molecular electrons

These two properties are needed in the cross section calculation. The kinetic energies of the molecular electrons were calculated using the HF method because one-electron properties calculated using HF calculations are variationally stable to first order. All ionization potentials used were vertical ionization potentials (VIP); i.e., they were calculated at the equilibrium geometry of the neutral molecule. Based on Koopmans theorem (*12*), VIPs can be estimated from the orbital energies in a HF calculation. The VIP of the outermost valence electron, called the First VIP, can also be calculated as the difference between the energies of the ion and the neutral molecule using higher order methods that include electron correlation such as MP2 and the CCSD(T) method (couple-cluster singles and doubles with perturbation treatment of triples) (*16,17*). Such treatment provides a more reliable value of the First VIP. In this paper, the MP2 method is used for DNA functional groups and the CCSD(T) method is used for water.

(c). Calculation of ionization cross sections

The iBED method was used in all cross section calculations. In the iBED formulation (*11*), the electron impact ionization cross section is given by the sum of two terms: (i) the Mott cross section of Coulomb scattering with exchange (*18*), modified by replacing the incident electron energy with the average energy from the binary encounter model (*19*), and (ii) the dipole Born cross section that describes the dipole interaction between the scattering electron and the target. While the modified Mott cross section describes the close collisions important at low electron energies, the dipole Born cross section describes the long range dipole interaction that dominates at high energies. Note, however, the dipole interaction potential used in the iBED formulation has a shielding term that describes the repulsive interaction as the scattering electron enters into the bonding region. This shielding term has been found to play an important role in obtaining reliable cross sections in electron collisions with radicals (*20,21*). The iBED formulation differs from the BEB model developed by Kim and Rudd (*7*) in several aspects. The BEB treatment uses the Bethe dipole cross section which represents the high-energy limit of the dipole interaction where only the long range dipole potential is important. The iBED treatment, on the other hand, not only describes the long-range electron-target dipole interaction, but also the shielding of the dipole field as the scattering electron comes inside the bonding region. In addition, in the iBED formulation the optical oscillator strength used in the dipole interaction depends on the ejected electron energy (E_p) as $E_p^{-3.5}$, an energy dependence derived by theoretical analysis (*11*). The BEB formulation, on the other hand, uses an E_p^{-3} energy dependence (*7*).

To determine the DI cross section, the ionization of an electron from a particular molecular orbital is calculated using the procedure described above. Next, the stability of the resulting cation with respect to dissociation is studied using quantum chemical methods. The cation is more likely to be unstable with respect to dissociation when the ionized electron comes from one of the inner orbitals. If the cation is unstable, the dissociation pathway(s) and the dissociation products are studied. The DI cross section yielding a specific set of dissociation products from a particular molecular orbital is the product of the ionization cross section from that orbital with the dissociation probability leading to the products in question. Note that the DI from one molecular orbital may

lead to more than one set of dissociation products. Similarly, the dissociation products may be produced from the DI of several molecular orbitals. In the latter case, the total DI producing the specific dissociation products will be the sum over the contributions from each molecular orbital.

3. Calculations and Results

(a). Total electron impact ionization cross section of water vapor

Cross section calculations of water were carried out at the experimental geometry of the isolated molecule (*22*). The VIPs of the three valence ionization channels $(1b_1)^{-1}$, $(3a_1)^{-1}$, and $(1b_2)^{-1}$, were determined using the CCSD(T) method and a correlation-consistent-polarized valence quadruple-zeta (cc-pVQZ) basis of Gaussian functions (*13,14*). The MOLPRO code (*23*) was used in the CCSD(T) calculations. In Table I, the VIPs for these three channels as well as the $(2a_1)^{-1}$ channel are compared with the tabulated experimental values of Levin and Lias (*24*) and the VIPs used in an earlier BEB calculation (*25*).

As an illustration of the quality of the data generated by the iBED method, Fig. 1 presents the total ionization cross section of water, $H_2O + e \rightarrow 2e +$ all products, calculated using the iBED method, the BEB method and the experimental data of Straub *et al*. (*26*) and Schutten *et al*. (*27*). The measurements of Straub *et al*. are considered the most accurate among available data, with an estimated error of ±5%, whereas the older data by Schutten *et al*., with an estimated error of ±15%, extend to higher energies. Two sets of iBED cross sections are presented, one with the optical oscillator strength f_o taken from the photoionization data of Brion *et al*. (*28*), and the second with f_o determined using the Thomas-Reich-Kuhn sum rule. The two iBED cross sections are in agreement with each other to within 10% on the low energy side; at the high energy side the difference is larger. They are also in agreement with both sets of experimental data. While the calculations using experimental f_o are in better overall agreement with experiment, the cross sections calculated with the Thomas-Reich-Kuhn sum rule are sufficiently accurate to provide useful data. Since photoionization measurements are not available for the DNA functional groups, the Thomas-Reich-

Kuhn sum rule approach provides a handle in the ionization calculations. The BEB cross sections calculated using the same set of molecular electron kinetic energies and VIPs as the iBED calculations are found to be ≈20% larger than both the iBED cross sections and experimental measurements at the peak of the cross section curve. An earlier BEB calculation (*25*) gives somewhat lower cross sections compared with the present BEB cross section, mainly due to the use of larger VIPs determined using the more approximate HF method. More details of the ionization and dissociative ionization study of H_2O and comparison with other available experimental data will be presented elsewhere (*29*).

(b). Total electron impact ionization cross sections of deoxyribose, phosphate, and C_3'- and C_5'-deoxyribose-phosphate

The geometries of deoxyribose, phosphate, C_3'- and C_5'-deoxyribose-phosphate, were determined with the MP2 method and the cc-pVDZ basis of Gaussian functions (*13-15*) employing the *GAMESS* code (*30*). Due to the size of the molecules under study, the cc-pVDZ basis was used in these calculations instead of the larger cc-pVQZ basis used in water. Nevertheless, the cc-pVDZ basis used in the present set of calculations is larger than the 3-21G basis (*5*) and the 6-311G basis (*9,10*) used in previous studies. To simulate the electronegativity of phosphate in DNA, we use the anion structure $H_2PO_4^-$ instead of the neutral species. Figure 2 presents the structure of the phosphate ($H_2PO_4^-$, denoted as Ph^-), deoxyribose sugar ($C_5H_{10}O_4$) and two conformations of the sugar-phosphate backbone, C_3'- and C_5'-deoxyribose-phosphate ($C_5H_{10}O_7P^-$, denoted as C_3-Ph^- and C_5-Ph^-, respectively), depending on the location of the sugar–phosphate bond. In a previous study of an analog of the DNA backbone (with H replacing the two OH groups of the deoxyribose-phosphate fragment at the bonding sites to the base and to the phosphate at the C_3' position), Bernhardt and Paretzke (*5*) performed calculations in the presence of a Na^+ counter ion. Unlike the calculation of Bernhardt and Paretzke (*5*), a counter ion is not used in our wave function calculations of Ph^-, C_3'-Ph^- and C_5'-Ph^-. Thus the calculated First VIPs for these three species should be lower than the corresponding neutral species. For Ph^- the calculated First VIP using MP2/cc-pVDZ (MP2 method and cc-pVDZ Gaussian basis) is 4.9 eV. For C_3'- Ph^- and

C_5'-Ph^- they are both 5.7 eV. By comparison, the First VIP of deoxyribose, a neutral species, from the present calculation is 10.6 eV, significantly higher than the First VIPs of the anions. The First VIP of the sugar-phosphate backbone analog determined by Bernhardt and Paretzke using a sodium counter ion is 10.52 eV at the HF/3-21G level. Thus the present calculation gives too low a VIP for Ph^-, C_3'-Ph^-, and C_5'-Ph^- due to the use of anions without the presence of a counter ion. Nevertheless, the major conclusions drawn from these calculations, as discussed below, are expected to remain valid.

Figure 3 presents the ionization cross sections of Ph^-, deoxyribose, C_3'-Ph^- and C_5'-Ph^- using the iBED method. The close spacing of the cross sections for C_3'-Ph^- and C_5'-Ph^- suggests that the total ionization cross section is insensitive to the location of the Ph^--deoxyribose bond. However, the individual ionization channels corresponding to specific bond-breaking processes such as DI are expected to be more sensitive to the Ph^--deoxyribose bonding site. Future studies will address this issue. In addition, the sum of the Ph^- and deoxyribose cross sections are close to the C_3'-Ph^- and C_5'-Ph^- cross sections. This appears to indicate a building-up principle where the total ionization cross section can be obtained from summing the ionization cross section of individual DNA functional groups. Further tests of the building-up principle, including the use of stoichiometry and extension to nucleosides and nucleotides, are being carried out. A new set of calculations, currently in progress, that uses Na^+ as a counter ion confirms the validity of the building-up principle even when counter ions are used (*31,32*).

The present set of C_3'-Ph^- and C_5'-Ph^- total ionization cross sections using the iBED method are larger than the cross sections for the sugar-phosphate analog reported by Bernhardt and Paretzke by ≈ 50%. However, the present results cannot be directly compared with the study of Bernhardt and Paretzke (*5*) because they did not use the deoxyribose structure.

.

(c). Total electron impact ionization cross sections of DNA bases

The geometries of the four DNA bases guanine, adenine, thymine, and cytosine were determined with the MP2 method and the cc-pVDZ basis of Gaussian functions (*13,14*) employing the *GAMESS* code (*30*). The First VIP of the DNA bases from the

present calculations are presented in Table 2, together with the experimental data (*33-39*) and the values used by Bernhardt and Paretzke (*5*) and Mozejko and Sanche (*9*) in their theoretical calculations. The present set of First VIP data was determined using MP2 calculations. Figure 4 presents the total ionization cross sections of guanine, adenine, thymine, and cytosine calculated using the iBED formulation. Of the four DNA bases, the ionization cross section of guanine is the largest, then in decreasing order, adenine, thymine, and cytosine. The order is in accordance with the known propensity of oxidation of the four bases by ionizing radiation. The iBED cross sections are comparable to the BED cross sections of Mozejko and Sanche, and somewhat larger than the data of Bernhardt and Paretzke.

(d). Dissociative ionization cross sections of cytosine

The ionization cross sections presented in Sec. (2a) – (2c) are total cross sections for the process M + e → 2e + all products. The only uniquely identified product in the process is a new, ejected electron. All other products are unidentified. For example, in the case of water, the products including in the total ionization cross sections are H_2O^+, OH^+, H^+, H_2^+, O^+, OH, H, H_2, and O. Thus the total ionization cross section corresponds to the probability of an energy deposition process by δ-rays producing a new electron, but does not provide the information regarding the detailed nature of the damage on the biomolecule. As a result, it cannot be deduced from the total ionization cross section what is the next step in the damage process. For example, it is known that the guanine cation is reactive, but the cytosine cation is less so. However, a cytosine radical cation, with one hydrogen removed, may well be much more reactive than cytosine cation itself. The biochemical model that we plan to develop requires data for the individual ionization process, including detailed information of ionization products. As a step in developing the necessary data, calculations of the DI of cytosine from the $20a_1$ orbital have been carried out,

$$\text{Cytosine} + e \rightarrow 2e + (\text{Cytosine} - H1)^+ + H. \qquad (1)$$

Molecular orbital analysis shows that the $20a_1$ orbital is the dominant channel for the DI at the H1 position. The cation $(\text{Cytosine} - H1)^+$ produced, corresponds to the parent cation Cytosine^+ with a hydrogen atom from the H1 position removed. Figure 5

illustrates the H1 position in cytosine and presents the DI cross section. The threshold of this process is 16.9 eV, significantly higher than the First VIP of cytosine. By taking the ratio of the DI cross section in Fig. 5 with the total ionization cross section of cytosine in Fig 4, the percentage of ionization that results in the production of (cytosine-H1)$^+$ via DI of the $20a_1$ orbital is obtained. For example, at 100 eV incident electron energy, 4.7% of ionization results in (cytosine-H1)$^+$ through this DI process. Note that the DI of higher-lying molecular orbitals may also produce H atom. Thus the total probability of producing H atom is the sum of all such DI probabililes. This is the first study of DI processes in DNA damage. The biochemical reactions that may occur due to the subsequent reaction of (Cytosine – H1)$^+$ will be the subject of future studies.

A summary of our calculations is presented in Table 3.

4. Discussions

The first set of molecular data for the development of a biochemical model of DNA radiation damage is presented here. The iBED method used for the calculation of electron impact ionization cross sections is first validated with a calculation of the water ionization cross section. The method is then applied to calculate the total ionization cross sections of DNA functional groups including Ph^-, dexoyribose sugar, and two conformers of the sugar-phosphate backbone, C_3'-Ph^- and C_5'-Ph^-, and the four DNA bases. The calculations of the sugar, phosphate, and sugar-phosphate backbone series show that the ionization cross sections of the two sugar-phosphate backbones are very close to each other. Furthermore, the sum of the sugar and phosphate cross sections are within 10% of the sugar-phosphate backbone cross section. This evidence suggests that for certain processes in DNA, the interaction is localized and we can study the system by treating smaller fragments at higher levels of accuracy. This "building-up principle" if validated in future calculations, should expedite the development of the biochemical model.

Calculations of the total ionization cross sections of the four DNA bases show that guanine has the largest cross section, then in descending order, adenine, thymine, and cytosine. This order agrees with the experimental observed oxidation propensity of

the bases by ionizing radiation. The present set of cross sections for the DNA bases is somewhat larger than the BEB and DM cross sections of Bernhardt and Paretzke (*5*) and comparable to the cross sections of Mozejko and Sanche (*9*). The present study presents the first DI cross section of a DNA base. This type of detailed study of the ionization processes that tracks the nature of the molecular products will enable us to trace the sequential biochemical steps in the mechanism of radiation damage and develop a more rigorous biochemical model.

Acknowledgement

This research was supported by NASA Ames Research Center IR&D funding. CED and GDF were supported by NASA prime contract NAS2-00062.

References

1. H. Nikjoo, P. O. O'Neill, M. Terrissol, D. T. Goodhead, Quantitative modelling of DNA damage using Monte Carlo track structure method. *Radiat. Environ. Biophys.* **38**, 31-38 (1999).
2. H. Nikjoo, S. Uehara, I. G. Khvostunov, F. A. Cucinotta, W. E. Wilson, D. T. Goodhead, Monte Carlo track structure for radiation biology and space applications. *Physica Medica* **XVII** Suppl. 1, 38 – 44 (2001).
3. M. Awada and P. C. Dedon, Formation of the 1,N2-glyxal adduct of deoxyguanosin by phosphoglycolaldehyde, a product of 3'-deoxyribose oxidation in DNA, *Chem Res. Toxicol.* **14**, 1247-1253 (2001).
4. K. Senthikumar, F. C. Grozeme, F. Guerra, F. M. Bickelhaupt, and L. D. A. Siebbeles, Mapping the site for selective oxidation of guanines in DNA, *J. Am. Chem. Soc.* **125**, 13658-13659 (2003). I. Saito, T. Nakamura, K. Nakatani, Y. Yoshioka, K. Yamaguchi, and H. Sugiyama, Mapping of the hot spots for DNA damage by one-electron oxidation efficacy of GG doublets and GGG triplets as a trap in the long range hole migration, *J. Am. Chem. Soc.* **120**, 12686-12687 (1988),
5. Ph. Bernhardt and H. G. Paretzke. Calculation of electron impact ionization cross sections of DNA using the Deutsch-Märk and Binary-encounter Bethe formalisms, *Int. J. Mass Spectrom.* **223-224**, 599-611 (2003).
6. H. Deutsch, K. Becker, S. Matt, T.D. Märk, Theoretical determination of absolute electron-impact cross sections of molecules, *Int. J. Mass Spectrom.* **197**, 37-69 (2000).

7. Y.-K. Kim and M. E. Rudd. Binary-encounter-dipole model for electron-impact ionization, *Phys. Rev. A* **50**, 3954-3967 (1994).
8. For the chemical structure of 2'-deoxy-D-ribose, see Lehninger Principles of Biochemistry, Fourth Edition, by David L. Nelson and Michael M. Cox, (W.H. Freeman, 2005), Chapter 8.
9. P. Mozejko and L. Sanche, Cross section calculations for electron scattering from DNA and RNA bases, *Radiat. Environ. Biophys*. **42**, 201-211 (2003).
10. P. Mozejko and L. Sanche, Cross sections for electron scattering from selected components of DNA and RNA. *Radiat. Phys. Chem*. **73**, 77-84 (2005).
11. W. M. Huo, A convergent series representation of the generalized oscillator strength for electron-impact ionization and an improved Binary-Encounter Dipole model, *Phys. Rev. A* **64**, 042719-1 to 042719-16 (2001).
12. A. Szabo and N.S. Ostlund, *Modern Quantum Chemistry. Introduction to Advanced Electronic Structure Theory*. MacMillan, New York (1982).
13. T.H. Dunning, Jr., Gaussian basis sets for use in correlated molecular calculations. I. The atoms boron through neon and hydrogen, *J. Chem. Phys*. **90** 1007-1023 (1989).
14. R.A. Kendall, T.H. Dunning, Jr., and R.J. Harrison, Electron Affinities of the first-row atoms revisited. Systematic basis sets and wave functions, *J. Chem. Phys*. **96**, 6796-6806 (1992).
15. D.E. Woon and T.H. Dunning, Jr., Gaussian basis sets for use in correlated molecular calculations. III. The atoms aluminum through argon, J. Chem. Phys. **93**, 1358-1371 (1993).
16. J. D. Watts, J. Gauss, and R. J. Bartlett, Coupled-cluster methods with noniterative triple excitations for restricted open-shell Hartree-Fock and other general single-determinant reference functions. Energies and analytical gradients. *J. Chem. Phys*. **98** 8718-8733 (1993).
17. M. J. O. Deegan and P. J. Knowles, Perturbative corrections to account for triple excitations in closed and open shell coupled cluster theories, *Chem. Phys*. *Lett.* **227** 321-326 (1994).
18. N. F. Mott and H. S. W. Massey, *The Theory of Atomic Collisions*, 3rd Edition, (Clarendon Press, Oxford, 1965).
19. L. Vriens in *Case Studies in Atomic Physics,* edited by E. W. McDaniel and M. R. C. McDowell, (North-Holland, Amsterdam, 1969), Vol. 1, p. 335.

20. W. M. Huo, V. Tarnovsky, and K. H. Becker, Total electron-impact ionization cross-sections of CF_x and NF_x (x=1-3), *Chem. Phys. Lett.* **358**, 328-336 (2002).
21. W. M. Huo, V. Tarnovsky, and K. H. Becker, Electron-impact ionization cross-sections of SF_3 and SF_5, *Int. J. of Mass Spectrom.* **233**, 111-116 (2004).
22. http://webbook.nist.gov/chemistry/
23. MOLPRO is a package of ab initio program written by H.-J. Werner and P.J. Knowles with contributions from R.D. Amos, A. Bernhardsson, A. Berning, P. Celani, D.L. Cooper, M.J.O. Deegan, A.J. Dobbyn, F. Eckert, C. Hampel, G. Hetzer, T. Korona, R. Lindh, A.W. Lloyd, S.J. McNicholas, F.R. Manby, W. Meyer, M.E. Mura, A. Nicklass, P. Palmieri, R. Pitzer, G. Rauhut, M. Schütz, H. Stoll, A.J. Stone, R. Tarroni, and T. Thorsteinsson.
24. R. D. Levin and S. G. Lias, NBS Report No. NSRDS-NBS 71 (1982).
25. W. Hwang, Y.-K. Kim, and M. E. Rudd, New model for electron-impact ionization cross sections of molecules, *J. Chem. Phys.* **104**, 2956-2966 (1996).
26. H. C. Straub, P. Renault, B. G. Lindsay, K. A. Smith, and R. F. Stebbings, Absolute partial cross sections for electron-impact ionization of H_2O an D_2O from threshold to 1000 eV. *J. Chem. Phys.* **108**, 109-116 (1998). See also B. G. Lindsay and M. A. Mangan, Cross sections for ion production by electron collisions with molecules, in *Interaction of Photons and Electrons with Molecules* Y. Itikawa, ed. Landolt-Börnstein, New Series, Group 1, Vol. 17, Pt C (Sprinter-Verlag, Berlin, 2003).
27. J. Schutten, F. J. De Heer, H. R. Moustafa, A. J. H. Boerboom, and J. Kistemaker, Gross- and partial-ionization cross sections for electrons on water vapor in the energy range 0.1 – 20 keV, *J. Chem. Phys.* **44,** 3924-3928 (1966).
28. C. E. Brion and F. Carnovale, The absolute partial photoionization cross section for the production of the X^2B_1 state of H_2O^+, *Chem. Phys.* **100**, 291-296 (1985). W. F. Chan, G. Cooper, and C. E. Brion, The electronic spectrum of water in the discrete and continuum regions. Absolute optical oscillator strengths for photoabsorption (6-200 eV), *Chem. Phys.* **178**, 387-400 (1993).
29. W. M. Huo and C. E. Dateo, to be published.
30. http://www.msg.ameslab.gov/GAMESS/GAMESS.html.
31. W. Huo and C. Dateo, Electron-impact total ionization cross sections of DNA sugar-phosphate backbone and an additivity principle, Bull. Am Phys. Soc. **50**, 50 (2005).
32. W.M. Huo, G.D. Fletcher, and C.E. Dateo, to be published.

33. N. H. Hush and A. S. Cheung, Ionization potentials and donor properties of nucleic acid and bases and related compounds, *Chem. Phys. Lett.* **34**, 11-13 (1975).
34. B. I. Verkin, L. F. Sukodub, I. K. Yanson, Potentials of ionization of nitrogen bases of nucleic-acids, *Dokl. Akad. Nauk. SSSR* **228**, 1452-1455 (1976).
35. D. Dougherty, E. S.Younathan, R. Voll, S. Abdulnur, S. P. McGlynn, Photoelectron spectroscopy of some biological molecules, *J. Electron. Spectr. Relat. Phenom.* **13**, 379-393 (1978).
36. J. Lin, C. Yu, S.Pen, I. Akiyama, K. Li, L. K. Lee, P. R. LeBreton, Ultraviolet photoelectron studies of ground-state electronic structure and gas phase tautomerism of purine and adenine, *J. Am. Chem. Soc.* **102**, 4627-4631 (1980).
37. S. Peng, A. Padva, P. R. LeBreton, Ultraviolet photoelectron studies of biological purines – valence electronic-structure of adenine, *Proc. Natl. Acad. Sci. U.S.A.* **73**, 2966-8 (1976).
38. C. Lifshitz, E. D. Bergmann, B. Pullman, The ionization potentials of biological purines and pyramidines, *Tetrahedron Lett.* **8**, 4583-4586 (1967).
39. G. Lauer, G. W. Schäfer, and A. Schweig, Functional subunits in the nucleic acid bases uracil and thymine, *Tetrahedron Lett*. **16**, 3939-3942 (1975).

Table 1. VIP of four ionization channels of water[a].

Channel	Vertical ionization potential (eV)		
	Present	Hwang *et al*. (25)	Levin and Lias (24)
$(1b_1)^{-1}$	12.746	12.61[b]	12.61
$(3a_1)^{-1}$	14.987	15.57	14.75
$(1b_2)^{-1}$	19.097	19.83	18.74
$(2a_1)^{-1}$	32.61[b]	36.88	32.61

[a]Data are for an isolated water molecule.

[b]Experimental value, from Ref. 24.

Table 2. First VIP (eV) of DNA bases.

DNA base	First VIP (eV)			
	Present	Bernhardt & Paretzke (5)	Mozejko & Sanche (9)	Experiment
Guanine	7.99[a]	8.24[b]	7.77	8.24±0.03 (33), 8.0±0.2 (34) 7.85(35)
Adenine	8.47[a]	8.44[b]	8.26	8.44±0.03 (33), 8.48 (36,37) 8.3±0.1 (34), 8.9±0.1 (38)
Thymine	8.91[a]	9.14[b]	8.87	9.14±0.03 (33), 9.0±0.1 (34), 9.4±0.1 (38), 9.20 (35), 9.02 (39)
Cytosine	8.76[a]	8.94[b]	8.68	8.94±0.03 (33), 9.0±0.1 (34), 8.9±0.2 (38), 8.45 (35)

[a]MP2/cc-pVDZ calculation.

[b]Experimental data from Ref. 33.

Table 3. Summary of ionization cross section calculations

Molecule[a]	Ionization	Builiding-up Principle	Dissociative ionization
Water	Yes	NA[b]	No
Phosphate, $H_2PO_4^-$	Yes	NA	No
Deoxyribose sugar, $C_5H_{10}O_4$	Yes	NA	No
C_3`-deoxyribose-phosphate ($C_5H_{10}O_7P^-$)	Yes	Yes	No
C_5`-deoxyribose-phosphate ($C_5H_{10}O_7P^-$)	Yes	Yes	No
Guanine	Yes	NA	No
Adenine	Yes	NA	No
Thymine	Yes	NA	No
Cytosine	Yes	NA	Yes

[a] All calculations are carried out for the isolated molecule.

[b] Not applicable

Figure captions

Figure 1. Total single ionization cross-section of water vapor, $H_2O + e \rightarrow 2e +$ all products. The full curve shows iBED cross sections determined using the optical oscillator strength from the photoionization data of Brion *et al*. (*28*). The dot-dashed curve presents iBED results where the Thomas-Reich-Kuhn sum rule is used to determine the optical oscillator strength. BEB cross sections are given by the dotted curve. The experimental data of Straub *et al.* (*26*) are represented by circles and the data of Shutten *et al.* (*27*) are given by triangles.

Figure 2. Molecular structures of the phosphate anion ($H_2PO_4^-$), deoxyribose sugar ($C_5H_{10}O_4$), and two conformers of the sugar-phosphate backbone, C_3'- and C_5'-deoxyribose-phosphate.

Figure 3. Total electron impact ionization cross sections of the phosphate anion, deoxyribose, and two conformers of the sugar-phosphate backbone, C_3'- and C_5'-deoxyribose-phosphate, calculated using the iBED formulation. Also presented in the heavy dotted curve is the sum of phosphate and deoxyribose ionization cross sections.

Figure 4. Total electron impact ionization cross sections of the DNA bases guanine, adenine, thymine, and cytosine calculated using the iBED formulation.

Figure 5. Dissociative ionization cross section of the process Cytosine + e $\rightarrow$ 2e+ $(\text{Cytosine} - \text{H1})^+ + \text{H}$. The position of H1 in cytosine is also illustrated.

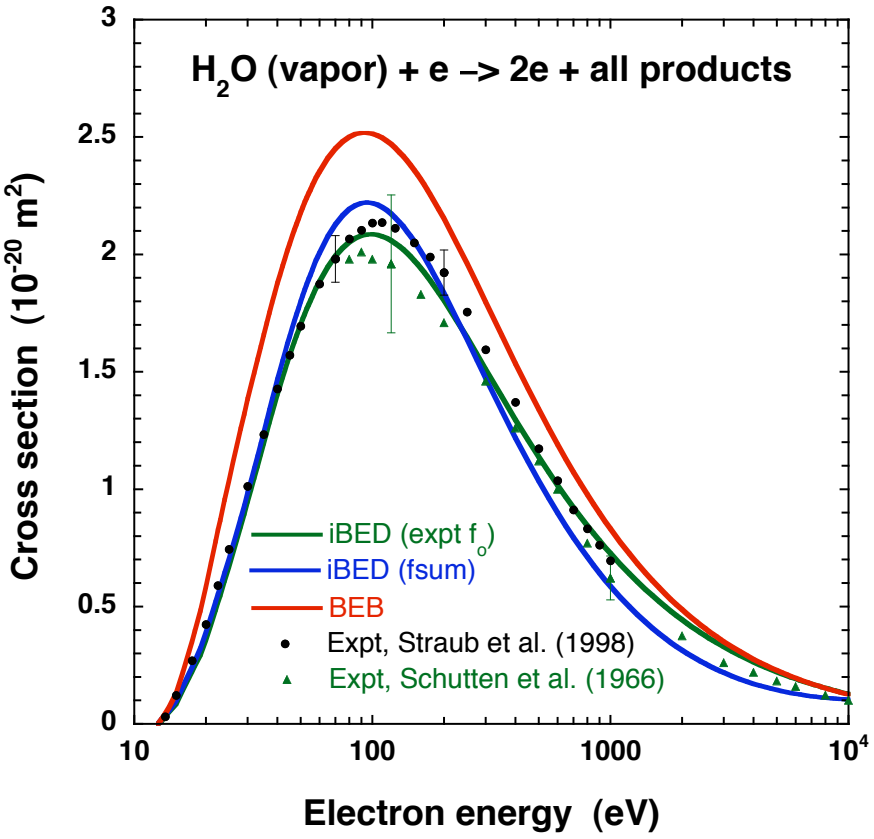
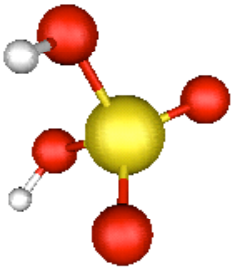
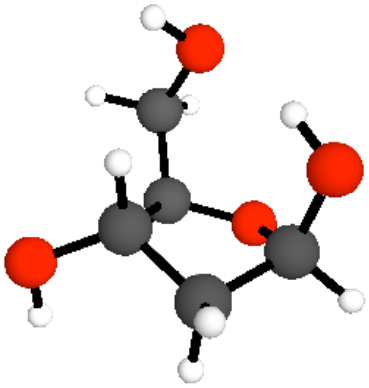

H2O (vapor) + e –> 2e + all products
Cross section (10-20 m2)
Electron energy (eV)
iBED (expt fo)
iBED (fsum)
BEB
Expt, Straub et al. (1998)
Expt, Schutten et al. (1966)
0
0.5
1
1.5
2
2.5
3
10
100
1000
10^4

Figure 1



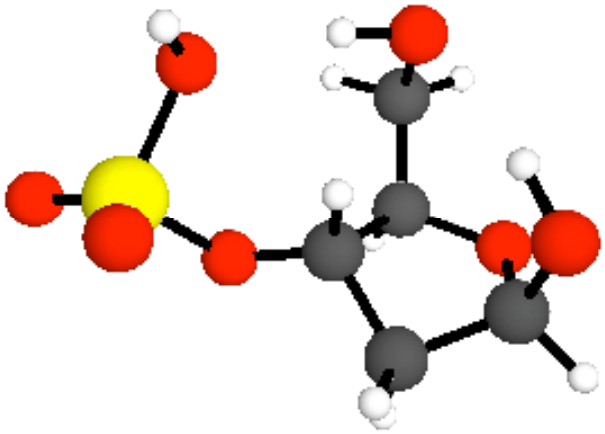
+



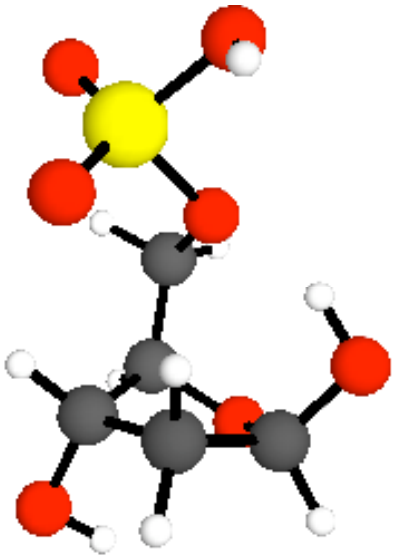
Phosphate
($H_2PO_4^-$)
Ph^-

Deoxyribose
($C_5H_{10}O_4$)

↓



and



C_3'—Ph^-
($C_5H_{10}O_7P^-$)

C_5'—Ph^-
($C_5H_{10}O_7P^-$)

Figure 2

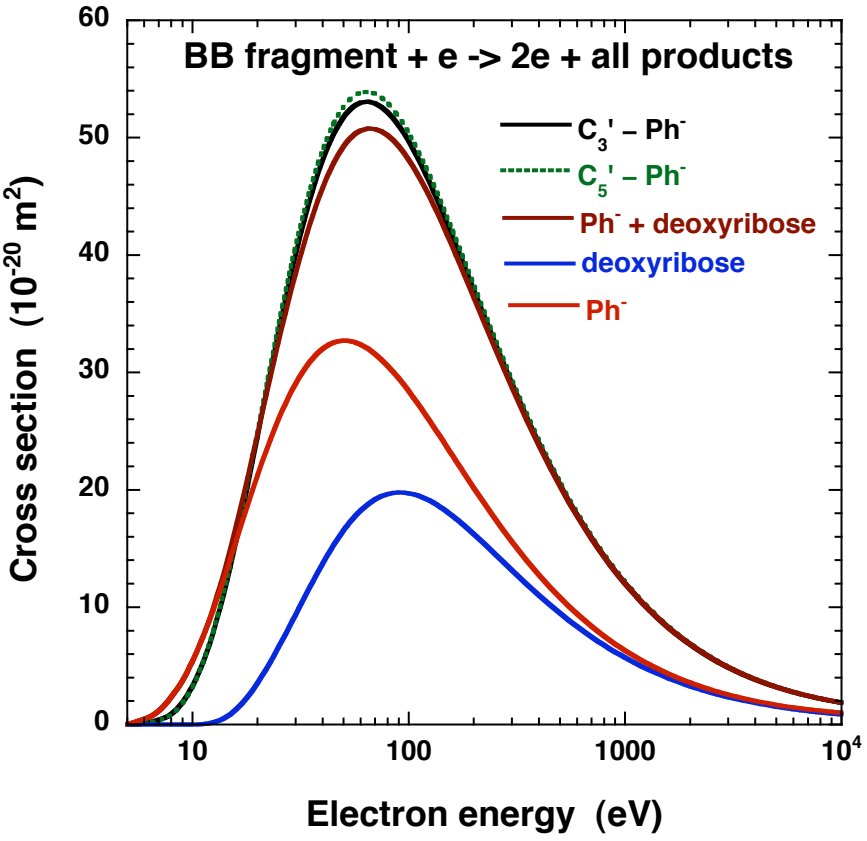

BB fragment + e -> 2e + all products
C3' – Ph-
C5' – Ph-
Ph- + deoxyribose
deoxyribose
Ph-
Cross section (10-20 m2)
Electron energy (eV)
0
10
20
30
40
50
60
10
100
1000
10^4

Figure 3

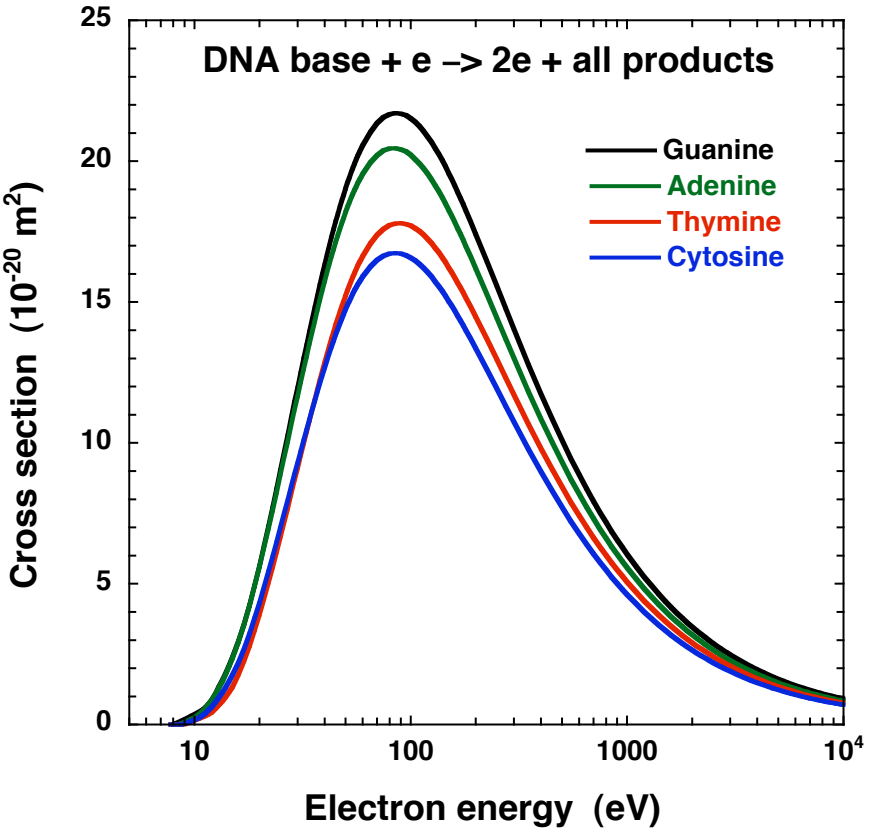

DNA base + e –> 2e + all products
Guanine
Adenine
Thymine
Cytosine
Cross section (10^-20 m^2)
Electron energy (eV)
0
5
10
15
20
25
10
100
1000
10^4

Figure 4

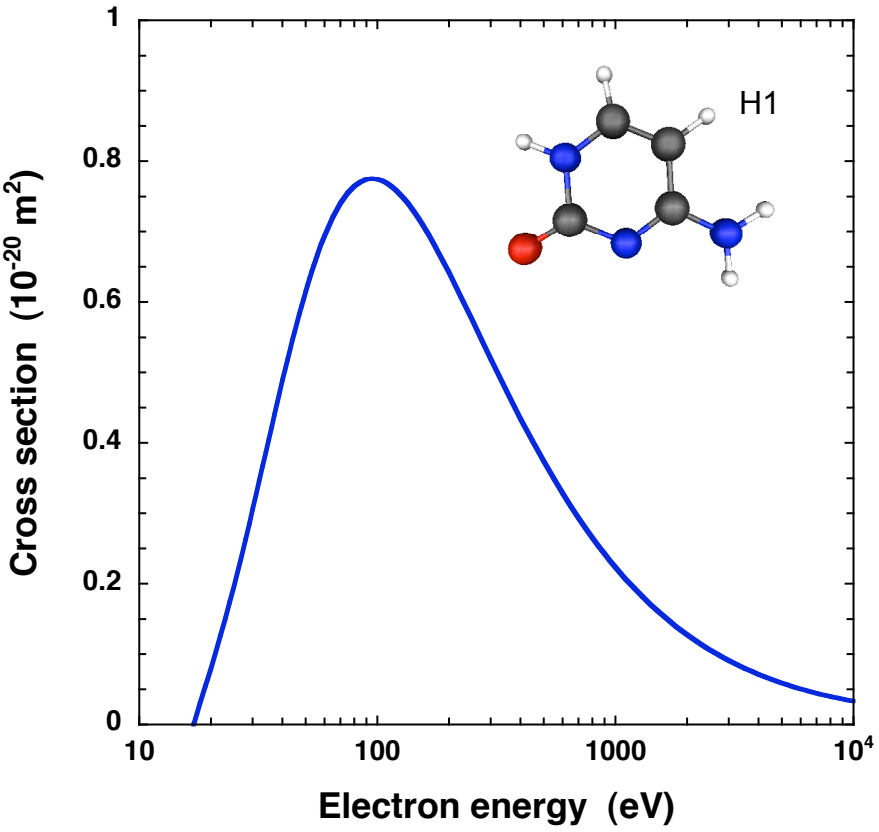

H1
Cross section (10^-20 m^2)
Electron energy (eV)
0
0.2
0.4
0.6
0.8
1
10
100
1000
10^4

Figure 5